Lasers in Manufacturing Conference 2021

Optical monitoring sensor system for laser-based directed energy deposition

Bohdan Vykhtar[a*], Alexander Marek Richter[a]

[a]*Fraunhofer IAPT, Am Schleusengraben 14, 21029 Hamburg, Germany*

Abstract

To achieve homogeneous material properties and thus high-quality components, a constant melt pool geometry and temperature are essential during the laser-based directed energy deposition processes. Especially at high deposition rates, process instabilities can appear, which lead to deviations in melt pool properties consequently resulting in the discrepancy in the target/actual comparison and, in the worst case, in the disposal of the component. To monitor the continuity of the melt pool properties, this paper presents an optical monitoring sensor system, which is capable of monitoring the process by guiding, filtering, and analyzing the optical signals of the melt pool. The presented sensor system is mounted on-axis to accomplish image acquisition and monitor the melt pool emissions but is also off-axis integrable in hybrid and wire-arc-based processes. The system is demonstrated for melt pool monitoring while processing stainless steel and an outlook is given on using that information to control the whole process.

Keywords: Real-Time Sensor, Additive Manufacturing, Monitoring; Robotics

1. Introduction

Additive Manufacturing (AM) processes are mainly used to generate complex three-dimensional components with high material utilization and a small carbon footprint compared to conventional manufacturing methods, Möller 2019. Especially robot-based AM processes, for instance, laser Directed Energy Deposition (DED), is gaining popularity in automation technology due to the high deposition rates and the potential to produce large parts. DED processes can be laser or arc-based and allow parts to be manufactured by melting metal material, shaped as wire or powder, Buhr 2020.

* Corresponding author. Tel.: +49 40 484010-786; fax: +49 40 48 40 10-780.

E-mail address: bohdan.vykhtar@iapt.fraunhofer.de.

To ensure consistent output of quality particularly during the laser-based DED processes, in-situ measuring methods are required, which can indicate the process stability.

With the use of various sensor systems such as pyrometers, IR cameras, Complementary Metal-Oxide Semiconductor (CMOS) cameras, or laser line and structured light scanners, melt pool properties, but also the built-up geometry can be monitored, Buhr 2020. This is achieved by analyzing the optical signals in the corresponding sensor system.

2. Optical sensing in laser-based DED processes

The optical signal monitoring of melt pool in laser-based DED processes can be implemented in the Visible Spectrum (VIS) or the Near Infrared (NIR) range. In the current state of the art, several researchers are investigating optical monitoring methods, to get a deeper understanding of the process and its optimization.

2.1. Optical monitoring of the melt pool in VIS

A common approach for a VIS in-situ monitoring of DED processes is the use of laser triangulation. Usually, those are set up on the off-axis to monitor the resulted 3D-printed surfaces or weld beads. This kind of monitoring setup was used by Heralić et al., 2012, to show, that the gathered data can be correlated to the process disturbances. They also utilized the data to develop an iterative learning closed-loop feedback controller, which can adjust the distance between the nozzle and the partly built object, to achieve homogeneous geometry. An improvement of this approach was developed by Buhr et al., 2020. Buhr was able to build a multidirectional laser triangulation setup, which allows the inspection of the building geometry and also to fulfill a closed-loop control using the generated 3D data across the moving process head. In further investigations, Buhr et al., 2018, identified the difficulty of inspecting the glowing material respectively the direct melt pool by a laser triangulation setup.

To investigate the properties of the melt pool, a camera-based monitoring system is used as an approach and the application of intelligent algorithms to the gathered data. In this manner, Wang et al., 2007, investigated the behavior of the melt pool of stainless steel 410 during laser-powder DED. To minimize the spectral emission of the process, optical filters were used with bandwidths of 700 nm to 800 nm and 800 nm to 900 nm. A field of view of nearly 25 mm x 25 mm was captured by the Charge Coupled Device (CCD) camera. Similar proceedings were performed by Kledwig et al., 2019. They investigated the melt pool characteristics by a coaxial monitoring system, which was integrated inside the DED machine. In this system, a dichroic mirror was used to decouple the VIS and project it through a bandpass filter of 740 nm onto the CCD-camera chip. For image analysis, a circular ROI was applied to the image, to identify the melt pool. In the next step, a threshold method was used to segment the melt pool. Further VIS camera-based approaches are observed by Doubenskaia et al., 2004, and Smurov et al. 2012, by monitoring the particle movement in powder-based DED processes.

2.2. Optical monitoring of the melt pool in NIR

NIR-high-speed cameras are often used to obtain the data of the melt pool. At the same time, it has the advantage of simultaneous capture the temperature of the observed melt pool. Zalameda et al., 2013, ensured the weld stability with a NIR camera during the wire-based DED process, while mounting the camera at a 60° angle to the weld pool. Hu et al., 2011, used this approach a achieve a stable powder feed rate in the DED process. Balu et al. used the high-speed IR camera to estimate the powder flux and speed. Their camera system was placed off-axis to the nozzle.

Another method of utilizing the NIR spectrum of the DED processes is the use of NIR photodiodes. Bono et al., 2017 developed a monitoring method, utilizing VIS and NIR photodiodes to correlate the resulting signals of the diodes with different types of weld anomalies. It was shown, that those anomalies consequently implied porosities, changes in penetration depths and changes in laser power, as well as poor joint preparation. Similar results were also presented by Shao et al., 2005. They correlated the photodiode signals to porosity and incomplete penetration of the material. This shows the wide operational range of photodiodes towards the multisensory approach in laser-based DED processes for a deeper understanding and mastering of those processes.

3. On-axis optical sensor system design

The current state of the art shows the necessity of a monitoring system, to obtain and process optical signals. In this work, the development of the sensor system is presented in Fig. 1, by adding additive manufacturing into the developing process of the optical-based in-situ sensors for melt pool monitoring in DED processes.

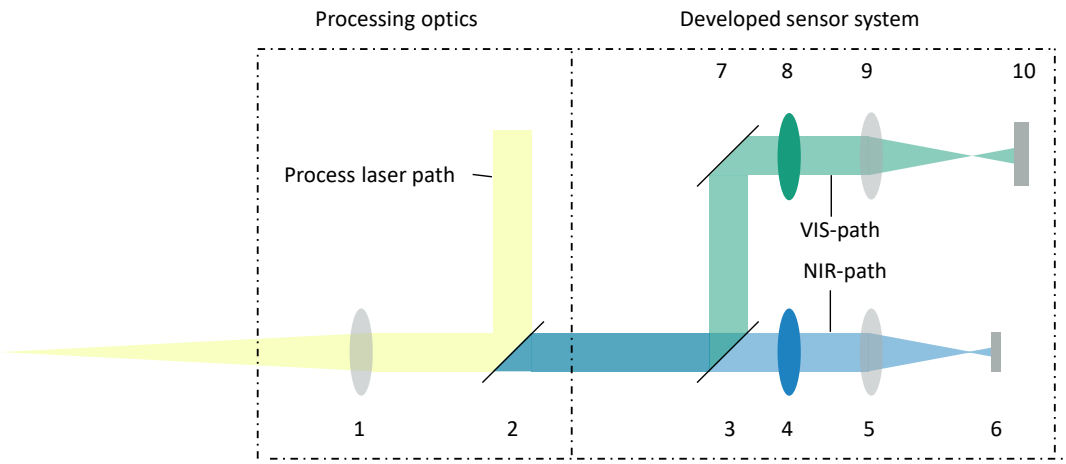

Fig. 1: Developed sensor system-scheme (right) mounted onto the processing optics (left). 1 – Focus lens; 2 – Dichroic mirror (1064 nm reflect only); 3 – Dichroic longpass mirror; 4 – Longpass filter; 5 – Focus lens; 6 – InGaAs photo diode; 7 – Silver mirror; 8 – Bandpass filter 685 nm; 9 – Focus lens; 11 – CMOS-Sensor

The presented sensor system was developed, to enable a wide range of applicability for optical melt pool monitoring in DED processes (on-axis and off-axis). A pre-requirement for on-axis integration of the developed sensor system is the optical configuration of the processing head. It shall be able to reflect the high-power laser source for the process and transmit the rest of the optical signal (VIS – NIR) to the sensor system at the sensor flange (2). Otherwise, mostly only VIS signals will be captured

The incoming optical signal through (2), emitted from the melt pool is split in the dichroic mirror (3) into the VIS (400 nm -700 nm) and NIR (700 nm – 2500 nm) path.

On the VIS path, a 685 nm bandpass filter with ±5 nm bandwidth and 85% transmission rate is positioned, to cut off the process emissions. The focusing lens (9) is configured in the way, that a 25 mm x 25 mm field of view results through the combination with the process focus lens (1). The resulting image is created by a 1280 px x 960 px USB3 CMOS-sensor with a framerate of 54 fps and a pixel size of 3,75 µm x 3,75 µm by a sensor size of 4,8 mm x 3,6 mm. This allows the geometrical in-situ melt pool monitoring.

On the NIR path, the light gets filtered by a long-pass filter, to cut off the remaining wavelength beneath 1100 nm, and to eliminate the possible rests of the laser emission. The light is focussed then on an InGaAs photodiode with a spectral sensitivity range of 900 nm to 2600 nm in a Ø1 mm active area. The peak sensitivity wavelength is 2300 nm. This enables the monitoring of the melt pool emissions.

The whole sensor system is built in a way, that further sensor elements can be inserted into the NIR and VIS paths, e.g. a VIS sensitive photodiode through a beam splitter between (7) and (8) or a NIR intensive camera in the NIR path.

With this approach, It was possible to combine the whole emission measurement in one sensor system, which is integrative in common processing optics, as well as the integration into lightning torch-based applications. For experimental purposes, the sensor system is demonstrated in section 5 regarding the analytics of the VIS path.

4. Experimental setup

The basic experimental setup is shown in Fig. 2. The developed sensor system was placed on the laser processing head, which has an optical interface to reflect the high-power laser light with the wavelength of 1025 nm to 1080 nm and transmits the rest of the optical signal through the optical mirror. The processing head with the sensor is mounted onto a Fanuc M-710iC/50 robot, which fulfills the kinematic movement. As a laser source for the process, a Fanuc fiber laser with 3KW was chosen with a wavelength of 1070 nm.

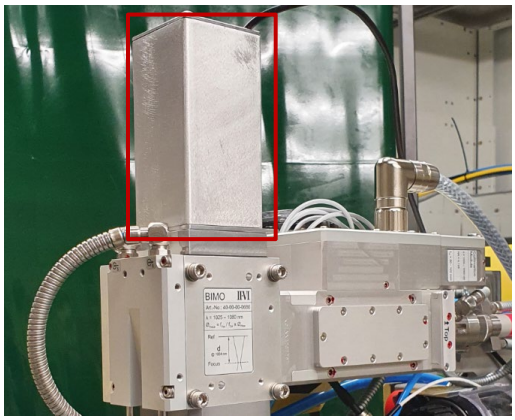

Fig. 2: Experimental set-up with the designed optical monitoring system showed in the red square

The designed sensor system is hulled to remove the optical environmental emissions. The wire is fed externally from the side, coupled to the processing optics. The process was set up with values from table 1. Several images were acquired during the process to develop the algorithm and to test the designed sensor system. The handling of the image data is given in the next section and the computation results are presented.

Table 1: Chosen process parameter to process stainless steel and to obtain optical data

Laser Power	Wire feed rate	Wire size Ø	Kinematic speed	Camera Exposure
$1500\ W$	$1{,}8\ m/min$	$1{,}2\ mm$	$1{,}8\ m/min$	$20\ \mu s$

5. Optical data processing and experimental application of developed sensor system

This paper presented the developed sensor system design for melt pool monitoring of DED processes. The focus of the experimental application and optical data processing is set to the VIS application of the sensors. In the following, the data handling and first results obtained by the developed sensor system are showed.

5.1. Processing of obtained VIS-data

The developed detection of the melt pool is divided into several sections and is settled on the described state of the art in section 2. First, the image is blurred by the Gaussian Blur. This suppresses the image noise and facilitates segmentation, Ohser 2018. The next step is to generate a histogram, which is an image operation that is performed independently of neighboring pixels and is, a method for evaluating statical data that is associated with lower computing power compared to other processing methods, Ohser 2018 and Priese 2015. With the help of this static data, threshold values for binarization can be obtained. The goal is to determine the threshold value, which leaves only the relevant and important image information.

In the following, two methods are presented that are particularly effective for capturing the threshold values from the histogram. The first thresholding method is based on the premise of a bimodal histogram, which has two maxima. To calculate the threshold the histogram has to be smoothed until only two local maxima remain. Here $h[k]$ is the current position of the histogram to be smoothed with $k = [0\ldots255]$ for an 8-bit gray value.

$$h(k) = \sum_{k}^{255} \frac{h(k-1) + h(k) + h(k+1)}{3} \tag{1}$$

The number of maxima is examined after each mean value smoothing. If there are more than two local maxima in the histogram, this smoothing process is reiterated until there are exactly two maxima left. If the smoothing was successful, the threshold value t is searched in the histogram. This is defined according to

$$h(t-1) > h(t) \leq h(t+1) \tag{2}$$

and is the minimum between the two local maxima, Prewitt 1966. A disadvantage of the Minimum Threshold method is that when using a non-bimodal histogram, this algorithm cannot find a threshold and hence aborts the calculation.

The second thresholding method is called Generalized Histogram Thresholding (GHT) and aims to be simple, fast, and effective. GHT operates by performing a maximum a posteriori estimation with a mixture of Gaussian and was invented by Barron, 2020. With the GHT it is possible to simulate the Otsu's thresholding, the Minimum Error Thresholding, and the Weighted Percentile Thresholding algorithm under certain conditions. Thus, the GHT allows interpolating between these three algorithms, which results in an improved thresholding accuracy. The GHT requires only 4 configurable parameters to generate the threshold value, which is listed in (3). This is called up with $GHT(x, n, \nu, \tau, \kappa, \omega)$ while $x = [0\ldots255]$ and n is the histogram. The parameters are defined as follows by default and can be adjusted, which leads for instance to higher sensitivity:

$$\nu, \kappa = \sum_{x}^{255} n(x) = 5.76e + 4 \qquad \tau = \sqrt{\frac{1}{12}} \qquad \omega = 0.5 \tag{3}$$

The now calculated threshold value can be traced with the help of a contour tracing, for which the Moore Neighborhood tracing algorithm is suitable, Gray 2003. This algorithm is particularly known for its reliability. In this paper, Moore Neighborhood tracing algorithm was modified to achieve faster computation results. In the modified version, the contour is tracked in the blurred image using the determined threshold. This way,

no binarization needs to be performed. Finally, the data is used to calculate the ellipse as an indicator of the melt pool geometry, which results in the quality of the melt pool. The analysis of the captured image series leads to the inference of the geometrical melt pool stability.

5.2. Results of experimental VIS data analysis

Figure 3a shows the acquired image by the developed sensor system. The movement direction of the actuator is from the top left corner to the bottom right corner in the image coordinates. The bright glowing melt pool also illuminates the created weld bead, which can be used for geometry analysis in the future. It can be also identified, that the process plume had an impact in form of a blur on the resulting image.

Nevertheless, the captured image through the developed monitoring system was blurred as shown in Fig. 3b by 3 x 3 Gaussian Blur kernel, following by the creation of the histogram of the image shown in Fig. 4a. In

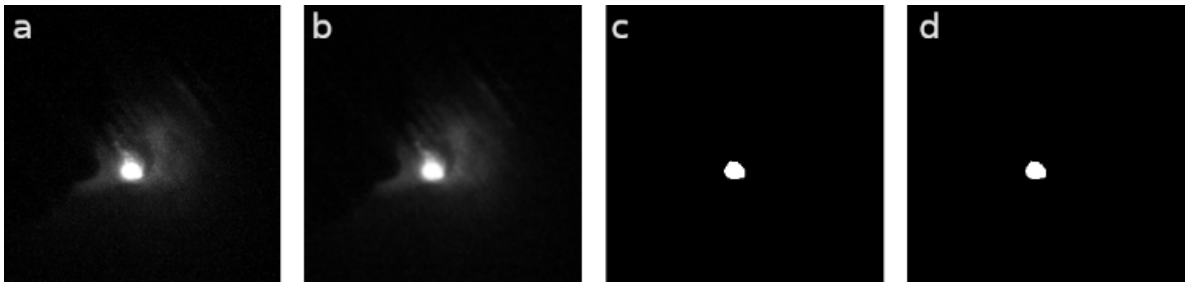

Fig. 3: (a) Source image; (b) Gaussian Blur; (c) theoretical binarization with Minimum Threshold; (d) theoretical binarization with GHT

the next step, both threshold determination methods were used and are shown for the illustration purpose binarized in Fig. 3c and Fig 3d. Fig. 3c represents the minimal threshold method. Fig. 3d shows the binarization of the image by selecting the parameters of GHT to $\omega = 1$ and $\tau = 90$. For optimization of each image, the threshold value can be shifted by the adjustment of τ.

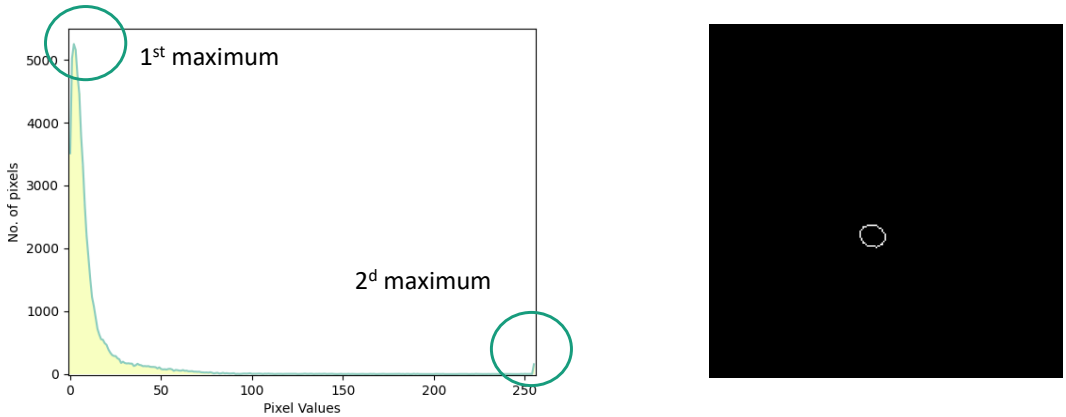

Fig. 4: (a) Histogram representation of the image; (b) Binarized Elipse drawing from the calculated data

In the next step, the contour is found by the modified Moor's Tracing algorithm to avoid the binarization procedure. For the calculation of the melt pool geometry, the algorithm fitEllipse by OpenCV was used. It

returns five values, including the axis length (a, b), the position in the image (x_0, y_0), and the angle θ in the corresponding image coordinate system, Fitzgibbon 1995.

In direct comparison, both threshold methods show only small deviations in the calculated ellipse. The minimum threshold method provides the values $t = 204$, $a = 16{,}53$; $b = 20{,}36$; $x_0 = 465{,}62$; $y_0 = 306{,}83$; and $\theta = 112{,}11$. While the values of the GHT method differ as follows: $t = 206$; $a = 16{,}18$; $b = 19{,}75$; $x_0 = 465{,}59$; $y_0 = 306{,}96$ and $\theta = 107{,}46$. Nevertheless, those values still represent only the parameter, coordinates, and orientation of the ellipse in image coordinates. To achieve absolute results, calibration is necessary. The ellipse of the melt pool is illustrated in Fig. 4b.

For on-axis integration of the developed sensor system, both algorithms performed quite similarly in the detection of the glowing melt pool. An important aspect of the algorithm is the execution time per frame. This has a direct impact on the possibility to control the process through the melt pool analysis. For the minimum threshold method, the time was calculated to 9500 µs and for the GHT 9889 µs on a Raspberry Pi 3 Model B. The single calculation times are listed in table 2.

Comparing both methods in determining the threshold value, the execution time of the minimum threshold is twenty-five times lower than the GHT threshold method. As can be seen in table 2, performing Gaussian blur and Histogram calculation on the whole image is an obvious bottleneck in the algorithm. This can be improved by using a Region of Interest (ROI), which will significantly reduce the computation time, which is demonstrated in table 2.

Table 2: Execution time of the algorithmic operation for melt pool monitoring

Method	Execution Time 1280x960 px	Execution Time 240x240 px
Gaussian Blur	$2870\ \mu s \pm 52\ \mu s$	$219\ \mu s\ \pm 40 \mu s$
Histogram	$6534\ \mu s\ \pm 30\ \mu s$	$314\ \mu s \pm 2\ \mu s$
Minimum Threshold	$14\ \mu s\ \pm 1\ \mu s$	$14\ \mu s \pm 1\ \mu s$
GHT	$403\ \mu s \pm 3\ \mu s$	$401\ \mu s \pm 3\ \mu s$
Moor's Tracing	$51\ \mu s \pm 2\ \mu s$	$49\ \mu s \pm 2\ \mu s$
OpenCV Ellipse fit	$301\ \mu s\ \pm 5\ \mu s$	$297\ \mu s \pm 5\ \mu s$
Total Minimum Threshold	$9500\ \mu s \pm 90\ \mu s$	$893\ \mu s \pm 50\ \mu s$
Total GHT	$9889\ \mu s \pm 92\ \mu s$	$1280\ \mu s \pm 52\ \mu s$

6. Summary and Outlook

This paper presented the optical sensor system design for DED applications and the use of the system in the laser-wire DED process. It was shown, that the sensor system with the determined optical components was able to capture melt pool emission for further processing of the digitalized data and can be used in the future as the new state-of-the-art tool to gather and process the optical signals in DED processes. For the determination of melt pool parameters, an algorithm was developed, which relied on the comparison of two different threshold determination methods. It was shown, that the computation time of the minimum threshold method is more than 25 times efficient than the GHT. Nevertheless, both algorithms computed similar results in determining the threshold value in the obtained images and therefore the calculation of the geometrical melt pool parameters.

The focus in further research will be relaying especially on sensor design for a smaller form factor as well as the data processing, especially in the investigation of the NIR-photodiode data. Further analytics of the obtained image data is required to calculate absolute values, which will base on a hand-eye calibration, to determine the transformation. On the algorithmic side, the automatic parameter detection for the threshold determination shall be researched, focused on the faster GHT method. Also, there is a need for the computation time of the Gaussian Blur, to achieve near real-time computation capabilities on edge devices. Further, the image series will be analyzed by storing the absolute values of the melt pool geometry and an in-situ comparison. With this, procedure it will be possible to detect irregularities and perform in-situ stabilization of the process through a closed-loop feedback controller.

References

Balu, P., Leggett, P. and Kovacevic, R., 2012. Parametric study on a Coaxial multi-material powder flow in laser-based powder deposition process. Journal of Materials Processing Technology, Vol. 212 No. 7, pp. 1598-1610.

Barron, J., 2020. A Generalization of Otsu's Method and Minimum Error Thresholding, Google Research, p.1-22

Bono, P., D., Allen, C., Angelo, G., Cisi, A., 2017. Investigation of optical sensor approaches for real-time monitoring during fibre laser welding J. Laser Appl. 29 022417

Buhr, M., Weber, J., Wenzl, J., P., Möller, M., Emmelmann, C., 2018. Influences of process conditions on stability of sensor controlled robot-based laser metal deposition. Procedia CIRP, Jg. 74, S. 149–153, 2018.

Buhr, M., Vykhtar, B., Emmelmann, C., 2020. Multidirectional Sensing for Digitalization in Additive Manufacturing Applications, Fraunhofer Direct Digital Manufacturing Conference 2020.

Doubenskaia, M., Bertrand, P., Smurov, I, 2004. Optical monitoring of Nd:YAG laser cladding, Thin Solid Films, p. 477-485

Fitzgibbon, A., Fisher, A., 1995. A buyer's guide to conic fitting. In Proceedings of the 6th British conference on Machine vision (Vol. 2), BMVA Press, p. 513–522

Gray, L., 2003. A Mathematician Looks at Wolfram's New Kind of Science. Not. Amer. Math. Soc. 50, 200-211.

Heralić, A., Christiansson, A.-K., Lennartson, B., 2012. Height control of lasermetal-wire deposition based on iterative learning control and 3D scanning, Opt. Lasers Eng. 50 (9) 1230–1241.

Hu, X.D., Kong, F.Z. and Yao, J.H., 2011. Development of monitoring and control system for laser remanufacturing, Applied Mechanics and Materials, Vol. 44, pp. 81-85

Kledwig, C., Perfahl, H., Reisacher, M., Brückner, F., Bliedtner, J., Leyens, C., 2019. Analysis of Melt Pool Characteristics and Process Parameters Using a Coaxial Monitoring System during Directed Energy Deposition in Additive Manufacturing. Materials, 12(2), 308.

Möller, M., Vykhtar, B., Emmelmann, C., Li, Z., Huang, J., 2019. Sustainable Production of Aircraft Systems: Carbon Footprint and Cost Potential of Additive Manufacturing in Aircraft Systems. Hamburg, 2019.

Ohser, J., 2018. Angewandte Bildverarbeitung und Bildanalyse, Fachbuchverlag Leipzig im Carl Hanser Verlag, p.41, p.75

Prewitt, J., Mortimer, Mendelsohn, M., 1966. Annals of the New York Academy of Sciences 128, pp. 1035–1053

Priese,L., 2015. Computer Vision, Springer Berlin Heidelberg, p. 74

Shao, J., Yan, Y., 2005. Review of techniques for online monitoring and inspection of laser welding J. Phys.: Conf. Ser. 15 101–7

Smurov, I., Doubenskaia, M., Grigoriev, S., & Nazarov, A. (2012). Optical Monitoring in Laser Cladding of Ti6Al4V. Journal of Thermal Spray Technology, 21(6), 1357–1362

Wang, L., Felicelli, S., Craig, J., 2007. Thermal modeling and experimental validation in the LENS™ process. 18th International Solid Freeform Fabrication Symposium; Austin, TX.

Zalameda, J. N., Burke, E. R., Hafley, R. A., Taminger, K. M., Domack, C. S., Brewer, A., & Martin, R. E., 2013. Thermal imaging for assessment of electron-beam freeform fabrication (EBF3) additive manufacturing deposits. Thermosense: Thermal Infrared Applications XXXV.